Title: Identification of a VapBC Toxin-Antitoxin System in a Thermophilic Bacterium *Thermus thermophilus* HB27

Authors: Yuqi Fan, Takayuki Hoshino and Akira Nakamura.

Affiliation: Faculty of Life and Environmental Sciences, University of Tsukuba, 1-1-1 Tennodai, Tsukuba, Ibaraki 305-8572, Japan

Corresponding author: Akira Nakamura, e-mail: nakamura.akira.fm@u.tsukuba.ac.jp, Tel: +81-29-853-6637, Fax: +81-29-853-6637

Abbreviations

Dox	doxycycline
DTT	dithiothreitol
IPTG	isopropyl-β-D-thiogalactopyranoside
PAGE	polyacrylamide gel electrophoresis
PBS	phosphate-buffered saline
PMSF	phenylmethanesulfonylfluoride
RNase	ribonuclease
TA	toxin-antitoxin

Abstract

There are 12 putative toxin-antitoxin (TA) loci in the *Thermus thermophilus* HB27 genome, including four VapBC and three HicBA families. Expression of these seven putative toxin genes in *Escherichia coli* demonstrated that one putative VapC toxin TTC0125 and two putative HicA toxins, TTC1395 and TTC1705, inhibited cell growth, and co-expression with cognate antiotoxin genes rescued growth, indicating that these genes function as TA loci. *In vitro* analysis with the purified TTC0125 and total RNA/mRNA from *E. coli* and *T. thermophilus* showed that TTC0125 has RNase activity to rRNA and mRNA; this activity was inhibited by the addition of the purified TTC0126. Translation inhibition assays showed that TTC0125 inhibited protein synthesis by degrading mRNA but not by inactivating ribosomes. Amino acid substitutions of 14 predicted catalytic and conserved residues in VapC toxins to Ala or Asp in TTC0125 indicated that nine residues are important for its *in vivo* toxin activity and *in vitro* RNase activity. These data demonstrate that TTC0125-TTC0126 functions as a VapBC TA module and causes growth inhibition by degrading free RNA. This is the first study to identify the function of TA systems in *T. thermophilus*.

Keywords: *Thermus thermophilus;* toxin-antitoxin system; VapBC; ribonuclease

Introduction

The gram-negative bacterium *Thermus thermophilus*, which was isolated from a hot spring in Japan (Henne et al. 2004; Oshima and Imahori 1974), is an extremely thermophilic model organism, which can grow in temperatures up to 85 ºC. *T. thermophilus* belongs to the phylum *Deinococcus-Thermus*, a small group of bacteria that are highly resistant to environmental hazards (Griffiths and Gupta 2007). The genus *Thermus* is closely related to *Archaea* and the genus *Mycobacterium* in the phylogenetic tree (Omelchenko et al. 2005).

Toxin-antitoxin (TA) loci are widely distributed in chromosomes and plasmids of *Bacteria* and *Archaea* (Grønlund and Gerdes 1999; Makarova et al. 2009; Pandey and Gerdes 2005; Gerdes et al. 2005; Krupovic et al. 2013). The chromosomes of some of these bacteria contain several TA loci, especially in one of the *Mycobacterium* species, *M. tuberculosis*, which possesses the largest number of putative TA loci on its chromosome, accounting for 79 loci (Ramage et al. 2009). TA systems consist of two small genes that encode a low molecular weight toxic protein (toxin) which reacts with intracellular target molecules related to essential cellular processes, such as DNA replication, protein translation, membrane integrity, and cell wall synthesis (Bertram and Schuster 2014; Maisonneuve et al. 2013; Page and Peti 2016), and a cognate antitoxin protein or RNA that inhibits toxin activity. Initially, TA loci were reported to play a role in bacterial programmed cell death for maintaining plasmid stability by killing the daughter cells that failed to inherit the plasmids (Winther and Gerdes 2011), or for acting as antiviral factors (Hazan and Engelberg-Kulka 2004; Pecota and Wood, 1996). More recently, it was recognized that the toxins play roles in response to cellular stresses (Bertram and Schuster 2014), such as amino acid starvation and the presence of antibiotics (Fauvart et al. 2011; Gerdes et al. 2005; Maisonneuve and Gerdes 2014), and triggering bacterial persistence (Yamaguchi and Inouye 2011). The vast majority of TA systems in chromosomes of *Bacteria* and *Archaea* are not redundant, likely due to each system developing different responses to specific stresses (Wang and Wood 2011). Currently, TA systems are grouped into six classes according to the mechanisms used by the antitoxins to neutralize the activities of the toxins.

The type II TA system is composed of a stable toxin protein and an unstable antitoxin protein. Under normal growth conditions, the antitoxin neutralizes toxin activity by forming a stable protein complex. When an environmental stressor is present, the antitoxin protein is degraded via proteolysis such that the toxin is released from the protein complex and becomes active to target intracellular molecules, such as mRNA at the ribosomal A site (Christensen and Gerdes 2003), initiator $tRNA^{fMet}$ (Winther and Gerdes 2011), Sarcin-Ricin loop of 23S rRNA (Winther et al. 2013), and glutamyl-tRNA synthetase (Germain et al. 2013), to inhibit cell growth or cause cell death. Most type II toxins function as RNases for degrading mRNA, either in a ribosome-dependent or independent manner (Unterholzner et al. 2014), such as MazF, Kid, ChpBK, MqsR, VapC, and HicA.

VapBC of the type II TA system is the most widely expanded TA family and its toxin, VapC, contains a PIN domain, which functions as a nuclease enzyme and cleaves single stranded RNA (Arcus et al. 2011). VapBC is often found in prokaryotic organisms, such as *M. tuberculosis*, one of the most devastating pathogenic bacteria,

which contains 45 VapBC loci (Arcus et al. 2011); however, most have not been well characterized until recently. The PIN domain consists of three highly conserved negatively-charged amino acids and is predicted to have RNase activity (Arcus et al. 2011). VapC toxins from different organisms were reported to have different target specificities; for example, VapC20 of *M. tuberculosis* inhibits translation by cleavage of 23S ribosomal RNA (Winther et al. 2013), and both VapC of *Shigella flexneri* and VapCLT2 of *Salmonella enterica* site-specifically cleave initiator tRNA (Winther and Gerdes 2011); on the other hand, VapC-mt4 of *M. tuberculosis* degrades mRNA (Sharp et al. 2012).

Little is known about HicAB, a novel Type II TA system family that was identified by Makarova et al. (2006). The *Escherichia coli* HicA toxin inhibits cell growth by mRNA degradation (Jørgensen et al. 2009), and the HicA from *Burkholderia pseudomallei* and *Pseudomonas aeruginosa* induces growth arrest and persistence in the presence of ciprofloxacin or ceftazidime (Butt et al. 2014; Li et al. 2016).

Despite many studies on mesophilic bacteria, including pathogens, the mechanisms and roles of TA systems in thermophilic microorganisms remain unknown. Based on the toxin-antitoxin database (Shao et al. 2011), 12 TA loci are predicted to be present in the *T. thermophilus* HB27 genome, of which seven are classified into known TA families, three (TTC1395-TTC1394, TTC1549-TTC1548, and TTC1705-TTC1704) in HicAB and four (TTC0113-TTC0114, TTC0125-TTC0126, TTC1207-TTC1208, and TTC1804-TTC1805) in VapBC; however, experimental analyses on these TA loci have not yet been reported. Here, we document the results of genetic analyses of these seven loci, and present detailed biochemical analyses of TTC0125-TTC0126.

Materials and methods

Bacterial strains, plasmids and media

T. thermophilus HB27 was used for genome isolation and purification of total RNA. *E. coli* strains DH5αZ1 (DH5α harboring *attB*:: P_{lacI^q}-*lacI*, P_{N25}-*tetR*, Sp^r; Lutz and Bujard 1997) and Rosetta (DE3) were used for plasmid construction and expression of toxin/TA genes from pZE21MCS2 (ColE1*ori*, $P_{LtetO-1}$, Kn^r; Lutz and Bujard 1997) and for production of TTC0125/TTC0126 proteins with pET28a, respectively. DH5αZ1 and pZE21MCS2 were purchased from Expressys. *T. thermophilus* and *E. coli* strains were cultured in TM medium (Koyama et al. 1986) at 70 °C and in LB medium at 37 °C, respectively.

Plasmid construction

To construct plasmids expressing the toxin genes or the TA modules under the control of a strictly regulated promoter, $P_{LtetO-1}$, each toxin gene or the TA locus was PCR-amplified with the primers listed in Table S1 from the *T. thermophilus* HB27 genome. Then, fragments were digested with *Kpn*I and *Sal*I, which were added just upstream of the initiation codon and downstream of the termination codon, respectively, and cloned into the respective sites of pZE21MCS2, using strain DH5αZ1 as a host.

For production and purification of the TTC0125 toxin and TTC0126 antitoxin, the TA locus and TTC0126 were PCR-amplified with primers TTC0126 F NdeI and TTC0125 R XhoI, and TTC0126 F NdeI and TTC0126 R XhoI, respectively. The resultant fragments were cloned into the respective sites of pET28a, giving rise to pET28-TTC0125-TTC0126 and pET28-TTC0126, respectively. In both plasmids, TTC0126 was fused in-frame with the 6xHis-tag in the vector at the N-terminus, and the *Xho*I site was located just downstream of the termination codon of TTC0125 of pET28-TTC0125-TTC0126 and TTC0126 of pET28-TTC0126.

The TT_P0042 gene encoding a β-glycosidase was PCR-amplified and cloned into pET28a, giving rise to pET28-TTP0042. This plasmid was used for *in vitro* transcription and translation assays. The *tetR* gene from *E. coli* was also cloned into pET28a to construct pET28-tetR, and used for *in vitro* transcription and RNase assays.

All plasmid constructs were confirmed by nucleotide sequencing with a CEQ8000XL DNA sequencer (Beckman-Coulter).

Growth inhibition assay

The strain DH5αZ1 harboring the pZE21MCS2 plasmid containing each toxin gene or TA locus was cultured in liquid LB medium with 50 μg/mL of kanamycin at 43 ºC. When the $O.D._{600}$ of the culture reached approximately 0.2, 100 ng/mL doxycycline (Dox) was added to induce gene expression. Cell growth was monitored periodically by measuring $O.D._{600}$. Three independent experiments were performed.

Purification of TTC0125 and TTC0126

The TTC0125 toxin was purified according to Winther and Gerdes (2011). *E. coli* Rosetta (DE3) harboring pET28-TTC0125-TTC0126 was cultured in LB medium supplemented with 50 μg/mL kanamycin and 20 μg/mL chloramphenicol at 30 °C. When $O.D._{600}$ reached 0.5, 0.2 mM IPTG was added, and, after further culturing for 5 h, cells were collected by centrifugation at 5000 x g for 10 min at 4 °C. Then, the cells

were re-suspended in ice-cold Lysis buffer (50 mM NaH_2PO_4, 100 mM NaCl, 20 mM imidazole, 0.5 mM PMSF (SIGMA), pH 7.4), and disrupted by sonication. After the cell debris were removed by centrifugation at 10,000 x g for 20 min at 4 ºC, a Ni-NTA agarose resin (Qiagen) was added to the supernatant and incubated for 2 h at 4 ºC, and subsequently loaded onto a gravity column. The column was washed extensively with Wash buffer (50 mM NaH_2PO_4, 100 mM NaCl, 20 mM imidazole, pH 7.4), and the protein complex of TTC0125-TTC0126 was eluted with Elution buffer (50 mM NaH_2PO_4, 100 mM NaCl, 200 mM imidazole, pH 7.4). Next, the protein complex was denatured by dialyzing the complex overnight at 4 ºC with Denaturation buffer (100 mM NaH_2PO_4, 10 mM Tris–HCl, 9.8 M Urea, pH 7.4), and the solution was again loaded onto a Ni-NTA agarose column. The denatured TTC0125 was eluted in the flow-through fraction, and refolded by the subsequent four-step dialysis against: (i) 1ⅹ PBS, 0.1 % Triton X-100, 5 mM DTT, (ii) 1ⅹ PBS, 5 mM DTT, (iii) 1ⅹ PBS, 5 mM DTT, and (iv) 1ⅹ PBS, 20 % glycerol, 1 mM DTT for 4 h in each dialysis.

For purification of TTC0126, *E. coli* Rosetta (DE3) harboring pET28-TTC0126 was cultured and the cell-free extract was prepared as previously described. TTC0126 was purified from the extract directly with a Ni-NTA agarose. The purification steps were monitored by SDS-PAGE according to Laemmli (1970).

RNA degradation assay

100 pmol of the purified TTC0125 protein, dialyzed against Reaction buffer (50 mM Tris-HCl, 100 mM NaCl, 10 mM $MgCl_2$, 1 mM DTT, pH 7.4) prior to the reaction, was incubated with 1 μg of total RNA from *E. coli* and *T. thermophilus*, which was prepared using a RNeasy Mini Kit (Qiagen), or an *in vitro*-transcribed *tetR* mRNA, which was prepared using pET28-tetR and an *in vitro* Transcription T7 Kit (TAKARA) and purified with RNeasy Mini Kit (Qiagen) kit, at 50 ºC in Reaction buffer. After 5, 15, 30, or 60 min of incubation, the reaction was stopped by adding 1x loading buffer (47.5 % formamide, 0.01 % SDS, 0.01 % bromophenol blue, 0.5 mg/ml EtBr, 0.5 mM EDTA) and placed on ice immediately. Then, the samples were loaded onto a denaturing agarose gel (1% agarose, 6.5% formaldehyde, 0.4 M MOPS, 100 mM sodium acetate, 10 mM EDTA) and analyzed. To test the inhibitory effect of TTC0126, 100 pmol of TTC0125 was incubated with 500 pmol of the purified TTC0126, which was also dialyzed against Reaction buffer, at 50 ºC for 15 min prior to the reaction, and used for the assay.

For measuring activity against intact ribosomes, ribosomes were purified from *E. coli* and *T. thermophilus* cells according to Pongs et al. (1973) and Trauner et al. (2011). Then, 10 μg of TTC0125 was incubated with 50 μg of ribosomes in Reaction buffer at 50 ºC for 60 min, and rRNA was purified with an RNeasy Mini Kit for gel electrophoresis.

For measuring activity against tRNA, the small RNA fraction containing tRNA was prepared from *E. coli* using ISOGEN II (NIPPON GENE). Then, 1 μg of the sample was incubated with TTC0125 as previously described, and resolved by an 8 % denaturing PAGE. After the sample was electroblotted onto a Hybond-N membrane, the initiator tRNA was hybridized with a biotin-labelled DNA probe, tRNAMet. Detection was conducted using a Chemiluminescent Nucleic Acid Detection Module (Thermo) and an LAS-2000 detector (Fuji film).

***In vitro* translation inhibition assay**

An *in vitro* translation inhibition assay was performed under the following conditions, using the *in vitro* transcribed TT_P0042 mRNA, which was synthesized with pET28-TTP0042 as a template and the *in vitro* Transcription T7 Kit, and a PUREfrex 2.0 kit (GeneFrontier; Shimizu et al. 2001). For each condition, the amount of the purified TTC0125, TTC0126 proteins, and the template mRNA used were 45, 270 pmol, and 2.5 μg, and the substrate-tRNA mixture (Solution I, PUREfrex), the enzyme mixture (Solution II), and the ribosome (Solution III) solutions used were 10, 1, and 2 μL in a total volume of 20 μL, respectively.

Condition 1. The template mRNA was incubated with TTC0125 at 37 ºC for 30 min. prior to *in vitro* translation.
Condition 2. The template mRNA was incubated with TTC0125 as previously described, then TTC0126 was added and the solution was further incubated for 15 min. After that, the translation reaction was started.
Condition 3. TTC0125 and TTC0126 were mixed and incubated at 37 ºC for 15 min. then the template mRNA was added and incubated further for 30 min. After that, the translation reaction was started.
Condition 4. The ribosome (Solution III) was incubated with TTC0125 at 37 ºC for 30 min. Then, the translation reaction was started by adding the template mRNA, Solution I and II.
Condition 5. The ribosome was incubated with TTC0125 as previously described, then TTC0126 was added and the solution was further incubated for 15 min. After that, the translation reaction was started.
Condition 6. TTC0125 and TTC0126 were mixed and incubated at 37 ºC for 15 min, then the ribosome was added and incubated further for 30 min. After that, the translation reaction was started.

The *in vitro* translation reaction was performed at 37 ºC for 4 h, and the translated TT_P0042 protein, containing the 6xHis-tag at its N-terminus, was detected by Western blotting using an anti-His antibody (Qiagen) and an ECL Prime Western Blotting Detection kit (GE Healthcare). Detection was performed using an LAS-2000 detector (Fuji film).

Site-directed mutagenesis

Single amino acid-substitution mutants of TTC0125 were constructed using the pZE21MCS2 plasmid harboring TTC0125 and pET28-TTC0125-TTC0126 as templates, primers listed in Table S1, and a QuickChange site-directed mutagenesis kit (Agilent Technologies). The resultant pZE21MCS2 plasmids harboring the mutant TTC0125 were used for the growth inhibition assays, and pET28-TTC0125-TTC0126 harboring mutant genes were used for protein purification and biochemical assays, as previously described.

Results and discussion

Identification of functional TA loci through growth inhibition assays

In the *T. thermophilus* HB27 genome, seven TA loci were predicted to be known TA families in the toxin-antitoxin database (Shao et al. 2011). Similarity searches of these putative toxins with the validated toxins in the Uniprot database indicated low-to-moderate similarities. TTC0113, TTC0125, TTC1207, and TTC1804, classified in the VapC family, showed 24, 44, 12, and 13 % similarity to VapC of *Mycobacterium smegmatis* (VAPC_MYCS2) (McKenzie et al. 2012), and TTC1395, TTC1549 and TTC1705 showed 37, 13 and 42 % similarity to HicA of *E. coli* (HICA_ECOLI), respectively (Jørgensen et al. 2009). Likewise, their cognate antitoxins also showed similar results. TTC0114, TTC0126, TTC1208, and TTC1805 showed 24, 37, 18, and 47 % similarity to the VapB antitoxin of *M. smegmatis* (VAPB_MYCS2), and TTC1394, TTC1548, and TTC1704 showed 27, 35 and 27 % similarity to the HicB antitoxin of *E. coli*, respectively (HICB_ECOLI).

To test whether these seven TA loci are functional, the toxin genes were cloned with or without their cognate antitoxin genes into the plasmid pZE21MCS2 and expressed under the control of the $P_{LtetO-1}$ promoter in *E. coli*. This promoter is strictly regulated in the presence of the TetR repressor in strain DH5αZ1, and expression can be induced with the addition of Dox (Lutz and Bujard 1997). Strains harboring the plasmids were cultured at 43 °C and gene expression was induced when the $O.D._{600}$ of the culture reached approximately 0.2.

As shown in Fig. 1a, expression of one VapC (TTC0125) and two HicA (TTC1395, TTC1549) genes strictly inhibited cell growth, whereas the other toxin genes had almost no effect. The growth-inhibitory effects of the former three toxin genes were more evident at 43 °C compared to 37 °C (data not shown), indicating that these toxins are more active at higher temperatures. Moreover, the effects were canceled out by co-expression of their cognate antitoxin genes (Fig. 1b).

The method used is restricted by assay temperature, as an *E. coli* strain is used as the host. Therefore, we cannot exclude the possibility that the other four toxins may also possess toxin activities at higher temperatures, i.e. the growth temperature of *T. thermophilus*. However, we concluded that at least these three loci function as type II TA systems in *T. thermophilus*, and focused on the TTC0125/TTC016 locus for further analysis. As these genes are classified into the VapBC family, we hereinafter renamed TTC0125 and TTC0126 as *Tt*VapC and *Tt*VapB, respectively.

Purification of *Tt*VapC and *Tt*VapB

We adopted the method described by Winther and Gerdes (2011) for *Tt*VapC purification. The *Tt*VapBC protein complex was first purified from the cell extracts of *E. coli* Rosetta (DE3) harboring pET28-TTC0125-TTC0126 through affinity chromatography against the 6xHis-tag attached to the N-terminus of *Tt*VapB; the proteins were denatured with a 9.8 M urea treatment. Then, the sample was loaded to the Ni-NTA agarose column and *Tt*VapC was purified in a flow-through fraction. The purified *Tt*VapC was renatured by a step-wise dialysis, and *Tt*VapB was directly purified

by the affinity chromatography from the cell extract of strain Rosetta (DE3) harboring pET28-TTC0126.

The purified *Tt*VapC and *Tt*VapB showed single bands on SDS-PAGE, the size of which were 14.7 and 10.0 kDa, respectively (Fig. 2).

*Tt*VapC degrades free RNA but not tRNA or rRNA in intact ribosomes

VapC family proteins contain a PIN domain and function as RNases (Arcus et al. 2011). In order to assess the molecular function of *Tt*VapC, we first analyzed its RNase activity using total RNA isolated from both *E. coli* and *T. thermophilus* as substrates. As shown in Fig. 3ab, the major bands corresponding to 16S and 23S rRNA were gradually shifted to low molecular-weight fractions across incubation time with *Tt*VapC, indicating that *Tt*VapC degrades at least 16S and 23S rRNA from both organisms. This degradation was completely inhibited when *Tt*VapC was incubated with *Tt*VapB prior to the reaction, showing that *Tt*VapB functions as antitoxin.

Some VapC toxins show strict substrate-specificities towards rRNA and tRNA. For example, VapC20 of *M. tuberculosis* cleaves the Sarcin-Ricin loop of 23S rRNA in the intact ribosome (Winther et al. 2013), and VapC (MvpT) of *Shigella flexneri* cleaves the anticodon loop of the initiator tRNA (Winther and Gerdes 2011). To examine whether *Tt*VapC has such substrate-specificities, we first evaluated its activity toward intact ribosomes from *E. coli* and *T. thermophilus*. As shown in Fig. S1ab, *Tt*VapC did not cleave or degrade 16S or 23S rRNA from both organisms. In order to assess initiator tRNA cleavage, small RNA fraction from *E. coli* was used as a substrate and the tRNA was detected by Northern blot hybridization. *Tt*VapC also did not react with the initiator tRNA (Fig. S1c). However, *Tt*VapC degrades *in vitro*-transcribed mRNA of the *E. coli* gene (*tetR*) in the same manner as total RNA (Fig. 3c). These results strongly indicate that *Tt*VapC does not possess substrate- or sequence-specificity, rather it degrades free RNA, such as VapC6 of *Sulfolobus solfataricus* (Maezato et al. 2011), and those of some pathogenic bacteria (Daines et al. 2007; Ramage et al. 2009).

*Tt*VapC inhibits translation by degrading mRNA

To gain insights into the *in vivo* molecular function of *Tt*VapC, an *in vitro*-translation assay was conducted using a PURERex kit. In this assay, an *in vitro*-transcribed TT_P0042 mRNA was used as a template for translation and translated 6xHis-tagged protein was detected by Western blotting.

A control experiment (without *Tt*VapC addition) produced a band of ca. 50.8 kDa corresponding to the molecular weight of the TT_P0042 protein with a 6×His-tag (Fig. 4). When the mRNA was incubated with *Tt*VapC prior to translation, no band was observed; also, the band was not observed when *Tt*VapB was added after incubation of the mRNA with *Tt*VapC. As the TT_P0042 protein was successfully translated when the mRNA was incubated with the *Tt*VapBC complex, it seems likely that *Tt*VapC inhibits translation by degrading mRNA. However, pre-treatment of ribosomes with *Tt*VapC resulted in a reduction of the translated product; this reduction did not occur when *Tt*VapB was added to the ribosome-*Tt*VapC mixture before the translation reaction.

Therefore, this result was likely caused by active *Tt*VapC degradation of mRNA during translation reaction but not inactivation of ribosomes. Pre-incubation of ribosome with *Tt*VapBC did not affect translation efficiency. We therefore conclude that *Tt*VapC inhibits translation by degrading mRNA and thereby inhibiting cell growth.

Identification of functionally-important residues in *Tt*VapC

We conducted site-directed mutagenesis to identify catalytically-important residues of *Tt*VapC. An amino acid sequence alignment of *Tt*VapC with "reviewed" VapCs in the Uniprot database (Fig. S2) generated by the T-Coffee program (Notredame et al. 2000) indicated that some residues, including the putative catalytic residues in PIN proteins, D4, E40, and D99 in *Tt*VapC numbering, are conserved in all VapCs. In addition, some residues are conserved in several but not in all VapCs. We selected those residues, including the putative catalytic residues, and introduced single amino acid substitutions to Ala or Asp. The mutant genes were then introduced into *E. coli* DH5αZ1 on pZE21MCS2 and the growth inhibition assays were conducted.

As shown in Fig. S3, the E23A, T72A, L105D, and V108D mutants showed similar growth inhibition as the wild type *Tt*VapC gene, suggesting that these residues are not required for its toxin activity. The F71A mutant showed a weaker growth inhibition, suggesting that this residue may be required for this activity to some extent. In contrast, the D4A, E40A, A76D, G94D, G98D, D99A, S102D, D119A, and D124A mutants, including the mutants of the putative catalytic residues, had almost no effect on cell growth, demonstrating the importance of these residues for its *in vivo* toxin activity.

Since the three-dimensional structure of *Tt*VapC is currently unavailable, we developed a three-dimensional model using the Phyre2 program to gain insight into the structure-activity relationship of *Tt*VapC (Kelly et al. 2015). The Phyre2 program indicated that *Tt*VapC showed a 37 % identity with VapC30 of *M. tuberculosis* H37Rv (PDB No. 4xgr), and a model structure of the second to 128th amino acid of *Tt*VapC was constructed based on that of VapC30 with a 100 % confidence, indicating the accuracy of the model.

Mapping of the mutated residues on the model structure (Fig. 5a) indicated that the three putative catalytic residues, whose mutations led to complete loss of growth inhibition activity, are located in one place with nearly the same topologies and distances of the side chains with those of VapC30, possibly forming the catalytic center. The other residues whose mutations also resulted in complete or partial loss of activity, except for G94 and D124, are located around the putative catalytic center, suggesting that these residues are involved in substrate binding or structural maintenance of the putative catalytic center. In the case of G98, since the Gly residue acts as a helix breaker and this residue is located adjacent to one of the catalytic residues, D99, G98 may be required for correct positioning of D99; it remains unknown as to why the mutations of G94D and D124A lost growth inhibition activity. The E23, T72, L105, and V108 residues are located at the other side of the protein. Therefore, it is possible that mutations of these residues did not affect activity.

In order to examine the mutant proteins which lost growth inhibition activity biochemically, the proteins were purified using the same method as the wild type *Tt*VapC. As shown in Fig. 5b, all of the mutant proteins were purified as single bands. Since this purification method relies on the complex formation with *Tt*VapB, this result indicates that the mutations introduced did not affect binding to *Tt*VapB. As expected,

all mutants lost RNase activities against total RNA (Fig. 5c), and one of the mutants, D99A, also lost activity against mRNA (Fig. 3c) and translation-inhibition activity (Fig. 4).

In conclusion, we characterized seven putative TA loci in *T. thermophilus*, and found that the three loci, TTC0125-TTC0126, TTC1395-TTC1396, and TTC1705-TTC1706, function as a TA module, indicated by the *E. coli* growth-inhibition assay. Biochemical analysis indicated that *Tt*VapC catalyzes degradation of RNA and inhibits translation by degrading free mRNA, and *Tt*VapB inhibits its activity as the antitoxin. Nine catalytically-important residues in *Tt*VapC, including the three putative catalytic residues, were identified, most of which are located near the catalytic center of the three-dimensional model.

Most *vapBC* loci in microorganisms consist of a bicystronic operon but the *TtvapBC* locus is included in a gene cluster encoding metabolic enzymes related to the glyoxylate cycle. It is possible that the physiological function of *Tt*VapBC is related to this cycle.

References

Arcus VL, Mckenzie JL, Robson J, Cook GM (2011) The PIN-domain ribonucleases and the prokaryotic VapBC toxin-antitoxin array. Protein Eng Des Sel 24: 33–40

Bertram R, Schuster CF (2014) Post-transcriptional regulation of gene expression in bacterial pathogens by toxin-antitoxin systems. Front Cell Infect Microbiol 4:6

Butt A, Higman V, Williams C, Crump MP, Hemsley CM, Harmer N, Titball RW (2014) The HicA toxin from *Burkholderia pseudomallei* has a role in persister cell formation. Biochem J 459: 333–344

Christensen SK, Gerdes K (2003) RelE toxins from Bacteria and Archaea cleave mRNAs on translating ribosomes, which are rescued by tmRNA. Mol Microbiol 48: 1389–1400

Daines DA, Wu MH, Yuan SY (2007) VapC-1 of nontypeable *Haemophilus influenzae* is a ribonuclease. J Bacteriol 189: 5041–5048

Fauvart M, De Groote VN, Michiels J (2011) Role of persister cells in chronic infections: Clinical relevance and perspectives on anti-persister therapies. J Med Microbiol 60: 699–709

Gerdes K, Christensen SK, Løbner-Olesen A (2005) Prokaryotic toxin-antitoxin stress response loci. Nat Rev Microbiol 3: 371–382

Germain E, Castro-Roa D, Zenkin N, Gerdes K (2013) Molecular mechanism of bacterial persistence by HipA. Mol Cell 52: 248–254

Griffiths E, Gupta RS (2007) Identification of signature proteins that are distinctive of the *Deinococcus-Thermus* phylum. Int Microbiol 10: 201–208

Grønlund H, Gerdes K (1999) Toxin-antitoxin systems homologous with relBE of *Escherichia coli* plasmid P307 are ubiquitous in prokaryotes. J Mol Biol 285: 1401–1415

Hazan R, Engelberg-Kulka H (2004) Escherichia coli mazEF-mediated cell death as a defense mechanism that inhibits the spread of phage P1. Mol Genet Genomic 272: 227–234

Henne A, Brüggemann H, Raasch C, Wiezer A, Hartsch T, Liesegang H, Fritz HJ (2004) The genome sequence of the extreme thermophile *Thermus thermophilus*. Nat Biotechnol 22: 547–553

Jørgensen MG, Pandey DP, Jaskolska M, Gerdes K (2009) HicA of *Escherichia coli* defines a novel family of translation-independent mRNA interferases in bacteria and archaea. J Bacteriol 191: 1191–1199

Kelly LA, Mezulis S, Yates C, Wass M, Sternberg M (2015) The Phyre2 web portal for protein modelling, prediction, and analysis. Nat Protoc 10: 845–858

Koyama Y, Hoshino T, Tomizuka N, Furukawa K (1986) Genetic transformation of the extreme thermophile *Thermus thermophilus* and of other *Thermus spp.* J Bacteriol 166: 338–340

Krupovic M, Gonnet M, Hania WB, Forterre P, Erauso G (2013) Insights into dynamics of mobile genetic elements in hyperthermophilic environments from five new Thermococcus plasmids. PloS One 8: e49044

Laemmli UK (1970) Cleavage of structural proteins during the assembly of the head of bacteriophage T4. Nature 227: 680–685

Li G, Shen M, Lu S, Le S, Tan Y, Wang J, Li, M (2016) Identification and characterization of the HicAB toxin-antitoxin system in the opportunistic pathogen *Pseudomonas aeruginosa*. Toxins 8: 1–12

Lutz R, Bujard H (1997) Independent and tight regulation of transcriptional units in *Escherichia coli* via the LacR/O, the TetR/O and AraC/I1-I2 regulatory elements. Nucleic Acids Res 25: 1203–1210

Maezato Y, Daugherty A, Dana K, Soo E, Cooper C, Tachdjian S, Blum P (2011) VapC6, a ribonucleolytic toxin regulates thermophilicity in the crenarchaeote *Sulfolobus solfataricus*. RNA 17: 1381–1392

Maisonneuve E, Castro-Camargo M, Gerdes K (2013) (p)ppGpp controls bacterial persistence by stochastic induction of toxin-antitoxin activity. Cell 154: 1140–1150

Maisonneuve E, Gerdes K (2014) Molecular mechanisms underlying bacterial persisters. Cell 157: 539–548

Makarova KS, Grishin NV, Koonin EV (2006) The HicAB cassette, a putative novel, RNA-targeting toxin-antitoxin system in archaea and bacteria. Bioinformatics 22: 2581–2584

Makarova KS, Wolf YI, Koonin EV (2009) Comprehensive comparative-genomic analysis of type 2 toxin-antitoxin systems and related mobile stress response systems in prokaryotes. Biology Direct 4: 19

McKenzie JL, Duyvestyn JM, Smith T, Bendak K, Mackay J, Cursons R, Arcus VL (2012) Determination of ribonuclease sequence-specificity using Pentaprobes and mass spectrometry. RNA 18: 1267–1278

Notredame C, Higgins DG, Heringa J (2000) T-coffee: a novel method for fast and accurate multiple sequence alignment. J Mol Biol 302: 205–217

Omelchenko MV, Wolf YI, Gaidamakova EK, Matrosova VY, Vasilenko A, Zhai M, Makarova KS (2005) Comparative genomics of *Thermus thermophilus* and *Deinococcus radiodurans*: divergent routes of adaptation to thermophily and radiation resistance. BMC Evol Biol 5: 57

Oshima T, Imahori K (1974) Physiochemical properties of deoxyribonucleic acid from an extreme thermophile. J Biochem (Tokyo) 75: 179–183

Page R, Peti W (2016) Toxin-antitoxin systems in bacterial growth arrest and persistence. Nat Chem Biol 12: 208–214

Pandey DP, Gerdes K (2005) Toxin-antitoxin loci are highly abundant in free-living but lost from host-associated prokaryotes. Nucleic Acids Res 33: 966–76

Pongs O, Bald R, Erdmann VA (1973) Identification of chloramphenicol-binding protein in *Escherichia coli* ribosomes by affinity labeling. Proc Natl Acad Sci USA 70: 2229–2233

Ramage HR, Connolly LE, Cox JS (2009) Comprehensive Functional Analysis of *Mycobacterium tuberculosis* Toxin-Antitoxin Systems: Implications for Pathogenesis, Stress Responses, and Evolution. PLoS Genet 5: e1000767

Shao Y, Harrison EM, Bi D, Tai C, He X, Ou HY, Deng Z (2011) TADB: A web-based resource for Type 2 toxin-antitoxin loci in bacteria and archaea. Nucleic Acids Res 39: 606–611

Sharp JD, Cruz JW, Raman S, Inouye M, Husson RN, Woychik NA (2012) Growth and translation inhibition through sequence-specific RNA binding by *Mycobacterium tuberculosis* VapC toxin. J Biol Chem 287: 12835–12847

Shimizu Y, Inoue A, Tomari Y, Suzuki T, Yokogawa T, Nishikawa K, Ueda T (2001) Cell-free translation reconstituted with purified components. Nat Biotechnol 19: 751–755

Trauner A, Bennett MH, Williams HD (2011) Isolation of bacterial ribosomes with

monolith chromatography. PLoS One 6: e16273
Unterholzner SJ, Poppenberger B, Rozhon W (2014) Toxin-antitoxin systems. Bioengineered 5: 1–13
Vesper O, Amitai S, Belitsky M, Byrgazov K, Kaberdina AC, Engelberg-Kulka H, Moll I (2011) Selective translation of leaderless mRNAs by specialized ribosomes generated by MazF in *Escherichia coli*. Cell 147: 147–157
Wang X, Wood TK (2011) Toxin-antitoxin systems influence biofilm and persister cell formation and the general stress response. Appl Environ Microbiol 77: 5577–5583
Winther KS, Brodersen DE, Brown AK, Gerdes K (2013) VapC20 of *Mycobacterium tuberculosis* cleaves the sarcin-ricin loop of 23S rRNA. Nat Commun 4:2796
Winther KS, Gerdes K (2011) Enteric virulence associated protein VapC inhibits translation by cleavage of initiator tRNA. Proc Natl Acad Sci USA 108: 7403–7407
Pecota DC, Wood TK (1996) Exclusion of T4 phage by the hok / sok killer locus from plasmid R1. J Bacteriol 178: 2044–2050
Yamaguchi Y, Inouye M (2011) Regulation of growth and death in Escherichia coli by toxin-antitoxin systems. Nat Rev Microbiol 9: 779–90

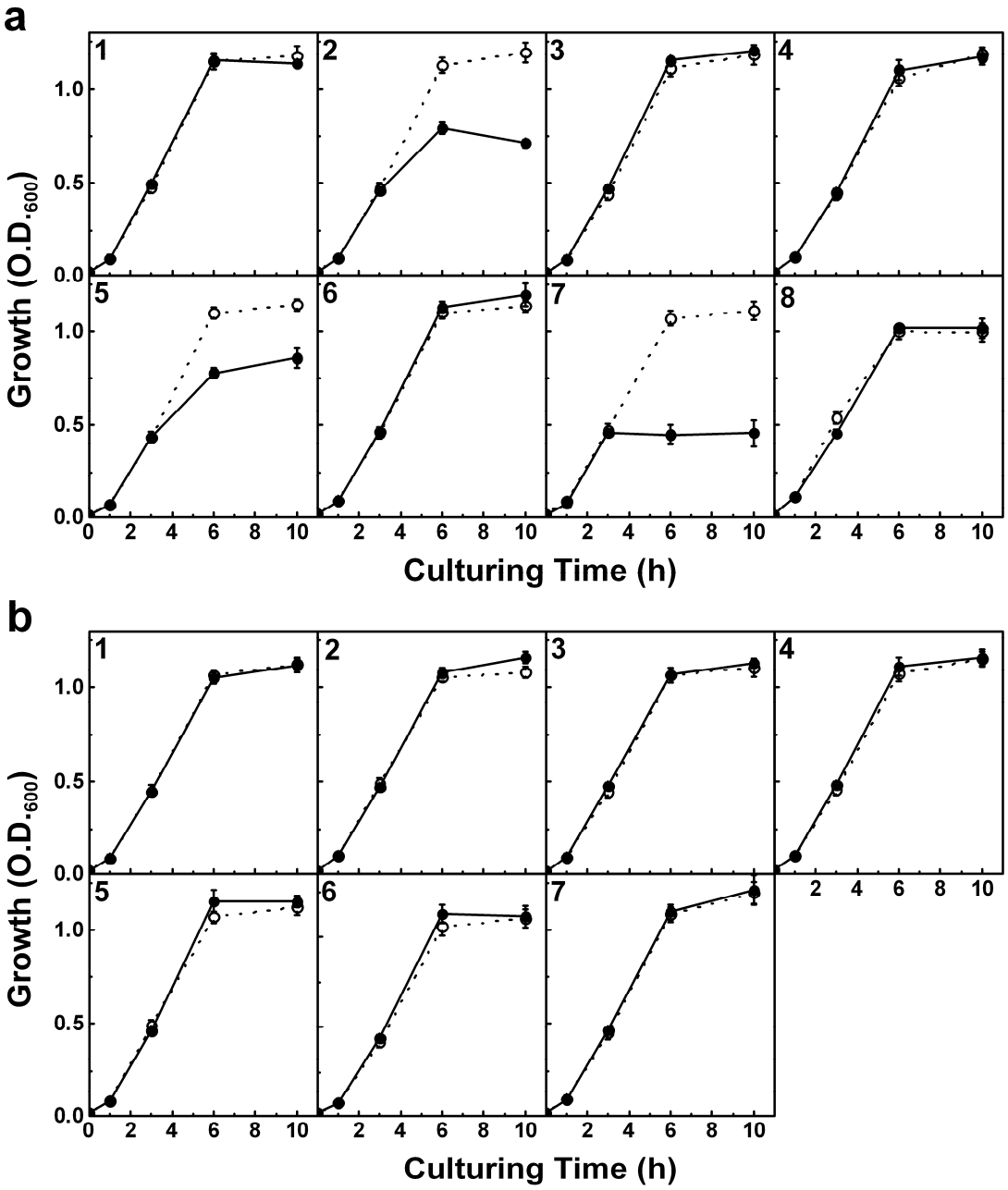

Fig. 1 Growth inhibition assay

E. coli DH5αZ1 harboring pZE21MCS2 containing toxin genes (**a**) of TTC0113 (**1**), TTC0125 (**2**), TTC1207 (**3**), TTC1804 (**4**), TTC1395 (**5**), TTC1549 (**6**), TTC1705 (**7**), or those with respective antitoxin genes (**b**) were cultured in LB medium containing kanamycin at 43 ºC; cell growth was monitored by measuring O.D.$_{600}$. At O.D.$_{600}$≈0.2, Dox was added to induce gene expression. Open circles with dotted lines indicate the culture without induction and filled circles with solid lines indicate the culture with induction. Panel (**8**) indicates the results from the strain harboring the vector plasmid. Culturing was conducted three times, and the mean values±standard deviations are shown.

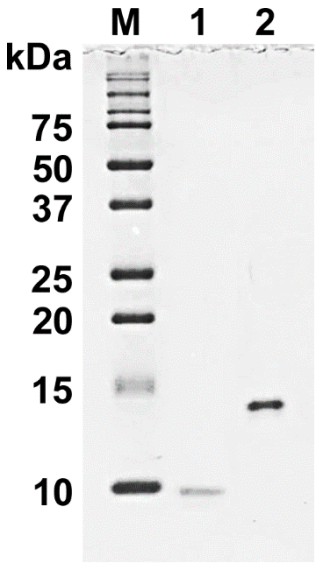

Fig. 2 SDS-PAGE of the purified *Tt*VapBC proteins
Lane M, molecular marker (in kDa); 1, *Tt*VapB; 2, *Tt*VapC.

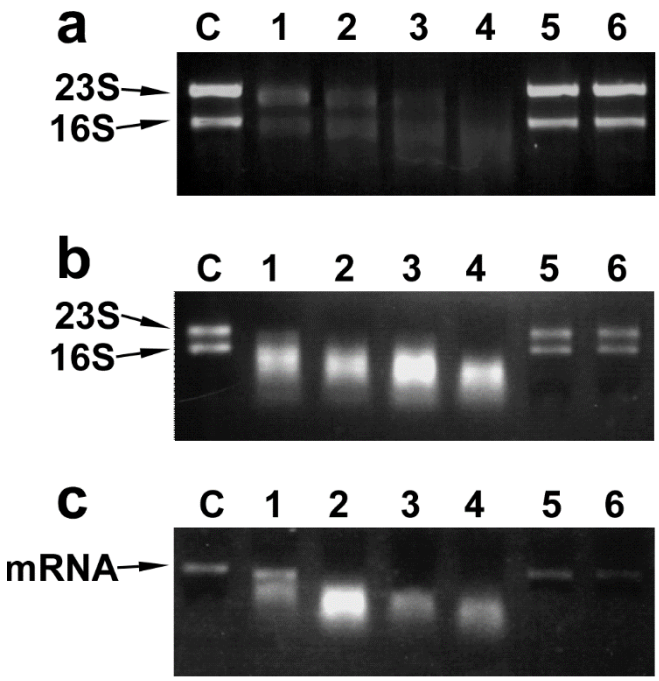

Fig. 3 RNA degradation assay
Total RNA from *E. coli* (**a**), *T. thermophilus* (**b**), and the *in vitro*-transcribed *tetR* mRNA (**c**) were incubated with the purified *Tt*VapC for 5 (lane 1), 10 (lane 2), 30 (lane 3), or 60 (lane 4) min, or incubated with the *Tt*VapBC complex (lane 5) or *Tt*VapC D99A mutant (lane 6) for 60 min and electrophoresed by denaturing agarose gel. Lanes C indicate the RNA samples without *Tt*VapC treatment, which were also incubated in Reaction buffer for 60 min. Positions of 23S, 16S rRNA, and mRNA are indicated by arrows.

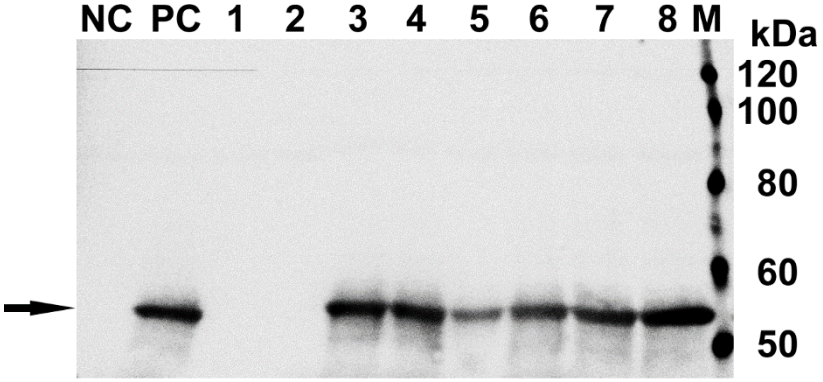

Fig. 4 *In vitro* translation inhibition assay
The *in vitro*-transcribed TT_P0042 mRNA or the *E. coli* ribosome fraction in the PURERex 2.0 kit were incubated with the *Tt*VapC or *Tt*VapBC complex, as described in Materials and methods, and *in vitro* translation reactions were conducted by adding other components of the kit. The translated product was resolved by SDS-PAGE and detected by Western blotting with an anti-His antibody. Lane 1, the mRNA was pre-incubated with *Tt*VapC (Condition 1); 2, the mRNA was pre-incubated with *Tt*VapC, and then *Tt*VapB was added (Condition 2); 3, the mRNA was pre-incubated with *Tt*VapBC complex (Condition 3); 4, the mRNA was pre-incubated with *Tt*VapC D99A mutant in Condition 1; 5, the ribosome was pre-incubated with *Tt*VapC (Condition 4); 6, the ribosome was pre-incubated with *Tt*VapC, and then *Tt*VapB was added (Condition 5); 7, the ribosome was pre-incubated with *Tt*VapBC complex (Condition 6); and 8, the ribosome was pre-incubated with *Tt*VapC D99A mutant in Condition 4. Lanes NC and PC indicate negative control without the template mRNA addition and positive control without *Tt*VapC treatment, respectively. Lane M indicates the molecular marker standards (MagicMark XP Western Protein Standard, Thermo Fisher Scientific), the size of which are indicated on the right. The bands corresponding to the full-length translated product is indicated by an arrow.

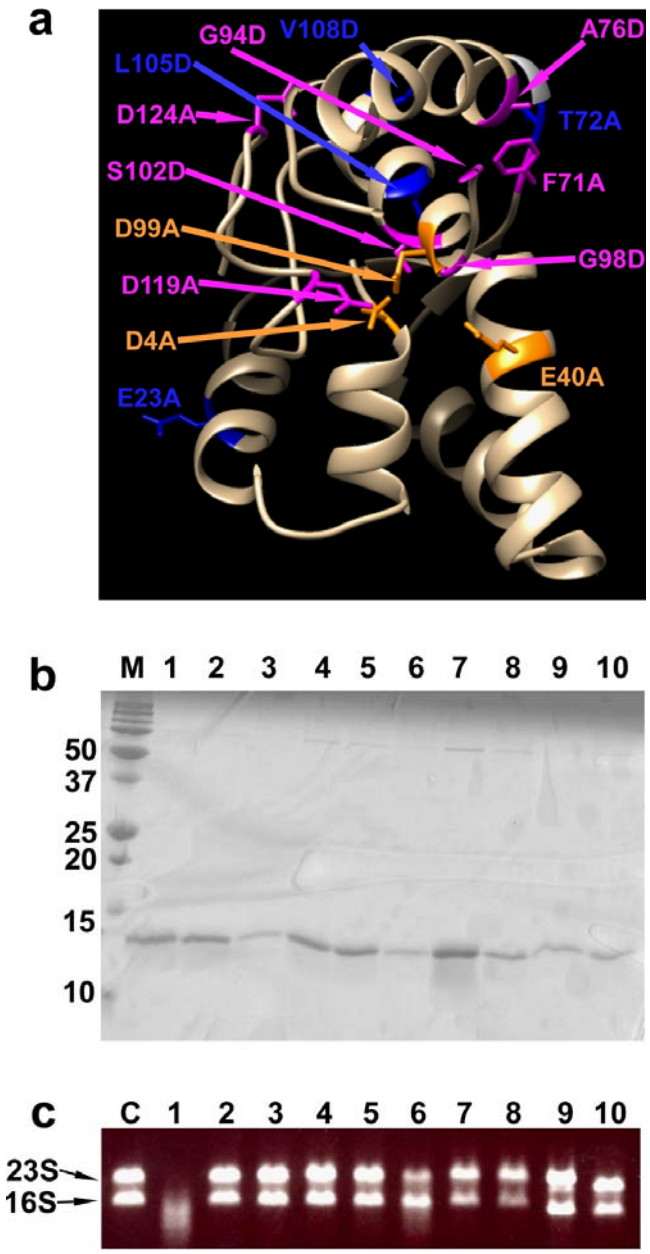

Fig. 5 Identification of catalytically-important residues of *Tt*VapC
(**a**) Three-dimensional model of *Tt*VapC constructed by the Phyre2 program. Residues to which the mutations were introduced are shown with side chains and introduced mutations are indicated. Residues whose mutations affected growth inhibition activity are shown in *orange* and *magenta*, of which *orange* residues indicate the putative catalytic residues. Those whose mutations did not affect the activity are shown in *blue*. (**b, c**) Purification (**b**) and RNA-degrading assay (**c**) of the purified *Tt*VapC mutants. Lane 1, wild type *Tt*VapC; 2, D4A; 3, E40A; 4, A76D; 5, G94D; 6, G98D; 7, D99A; 8, S102D; 9, D119A; 10, D124A mutants. Lanes M and C indicate molecular markers (in kDa) and a control experiment without *Tt*VapC incubation, respectively. RNA-degradation assays were conducted with *E. coli* total RNA, and the positions of 23S and 16S rRNA are indicated by arrows.